

Properties and Improved Space Survivability of POSS (Polyhedral Oligomeric Silsesquioxane) Polyimides

Sandra J. Tomczak⁽¹⁾, Darrell Marchant⁽²⁾, Steve Svejda⁽¹⁾, Timothy K. Minton⁽³⁾,
Amy L. Brunsvold⁽³⁾, Irina Gouzman⁽⁴⁾, Eitan Grossman⁽⁴⁾, George C. Schatz⁽⁵⁾, Diego Troya⁽⁵⁾,
LiPeng Sun⁽⁵⁾, Rene I. Gonzalez

⁽¹⁾ AFRL/PRSM, Materials Applications Branch, Air Force Research Laboratory, 10 E. Saturn Blvd,
Bldg. 8451, Edwards AFB, CA 93524, USA, *sandra.tomczak@edwards.af.mil

⁽²⁾ ERC Incorporated, Materials Applications Branch, Air Force Research Laboratory, 10 East Saturn
Blvd, Bldg 8451, Edwards AFB, CA 93524, USA

⁽³⁾ Department of Chemistry and Biochemistry, Montana State University, 108 Gaines Hall,
Bozeman, MT 59717, USA tminton@montana.edu

⁽⁴⁾ Space Environment Section, Soreq NRC, Yavne 81800, Israel

⁽⁵⁾ Department of Chemistry, Northwestern University, Evanston, IL. 60208-3113 USA,
schatz@chem.northwestern.edu

ABSTRACT

Kapton polyimide (PI) is widely used on the exterior of spacecraft as a thermal insulator. Atomic oxygen (AO) in lower earth orbit (LEO) causes severe degradation in Kapton resulting in reduced spacecraft lifetimes. One solution is to coat the polymer surface with SiO₂ since this coating is known to impart remarkable oxidation resistance. Imperfections in the SiO₂ application process and micrometeoroid / debris impact in orbit damage the SiO₂ coating, leading to erosion of Kapton.

A self passivating, self healing silica layer protecting underlying Kapton upon exposure to AO may result from the nanodispersion of silicon and oxygen within the polymer matrix. Polyhedral oligomeric silsesquioxane (POSS) is composed of an inorganic cage structure with a 2:3 Si:O ratio surrounded by tailorable organic groups and is a possible delivery system for nanodispersed silica. A POSS dianiline was copolymerized with pyromellitic dianhydride and 4,4'-oxydianiline resulting in POSS Kapton Polyimide. The glass transition temperature (T_g) of 5 to 25 weight % POSS Polyimide was determined to be slightly lower, 5 – 10 %, than that of unmodified polyimides (414 °C). Furthermore the room temperature modulus of polyimide is unaffected by POSS, and the modulus at temperatures greater than the T_g of the polyimide is doubled by the incorporation of 20 wt % POSS.

To simulate LEO conditions, POSS PI films underwent exposure to a hyperthermal O-atom beam. Surface analysis of exposed and unexposed films conducted with X-ray photoelectron spectroscopy, atomic force microscopy, and surface profilometry support the formation of a SiO₂ self healing passivation layer upon AO exposure. This is exemplified by erosion rates of 10 and 20 weight % POSS PI samples which were 3.7 and 0.98 percent, respectively, of the erosion rate for Kapton H at a fluence of 8.5 x 10²⁰ O atoms cm⁻². This data corresponds to an erosion yield for 10 wt % POSS PI of 4.8 % of Kapton H. In a separate exposure, at a fluence of 7.33 x 10²⁰ O atoms cm⁻², 25 wt % POSS Polyimide showed the erosion yield of about 1.1 % of that of Kapton H. Also, recently at a lower fluence of 2.03 x 10²⁰ O atoms cm⁻², in going from 20 to 25 wt % POSS PI the erosion was decreased by a factor of 2 with an erosion yield too minor to be measured for 25 wt % POSS PI.

INTRODUCTION

Kapton Polyimide is used extensively on spacecraft in flexible substrates for lightweight, high-power solar arrays because of its inherent strength, temperature stability, excellent insulation

DISTRIBUTION A. Approved for public release; distribution unlimited.

Report Documentation Page

Form Approved
OMB No. 0704-0188

Public reporting burden for the collection of information is estimated to average 1 hour per response, including the time for reviewing instructions, searching existing data sources, gathering and maintaining the data needed, and completing and reviewing the collection of information. Send comments regarding this burden estimate or any other aspect of this collection of information, including suggestions for reducing this burden, to Washington Headquarters Services, Directorate for Information Operations and Reports, 1215 Jefferson Davis Highway, Suite 1204, Arlington VA 22202-4302. Respondents should be aware that notwithstanding any other provision of law, no person shall be subject to a penalty for failing to comply with a collection of information if it does not display a currently valid OMB control number.

1. REPORT DATE

NOV 2004

2. REPORT TYPE

3. DATES COVERED

-

4. TITLE AND SUBTITLE

Properties and Improved Space Survivability of POSS (Polyhedral Oligomeric Silsesquioxane) Polyimides

5a. CONTRACT NUMBER

5b. GRANT NUMBER

5c. PROGRAM ELEMENT NUMBER

6. AUTHOR(S)

Sandra Tomczak; Darrell Marchant; Steve Svejda; Timothy Minton; Amy Brunsvold

5d. PROJECT NUMBER

DARP

5e. TASK NUMBER

A443

5f. WORK UNIT NUMBER

7. PERFORMING ORGANIZATION NAME(S) AND ADDRESS(ES)

Air Force Research Laboratory (AFMC), AFRL/PRSM, 10 E. Saturn Blvd., Edwards AFB, CA, 93524-7680

8. PERFORMING ORGANIZATION REPORT NUMBER

9. SPONSORING/MONITORING AGENCY NAME(S) AND ADDRESS(ES)

10. SPONSOR/MONITOR'S ACRONYM(S)

11. SPONSOR/MONITOR'S REPORT NUMBER(S)

12. DISTRIBUTION/AVAILABILITY STATEMENT

Approved for public release; distribution unlimited

13. SUPPLEMENTARY NOTES

14. ABSTRACT

Kapton polyimide (PI) is widely used on the exterior of spacecraft as a thermal insulator. Atomic oxygen (AO) in lower earth orbit (LEO) causes severe degradation in Kapton resulting in reduced spacecraft lifetimes. One solution is to coat the polymer surface with SiO₂ since this coating is known to impart remarkable oxidation resistance. Imperfections in the SiO₂ application process and micrometeoroid / debris impact in orbit damage the SiO₂ coating, leading to erosion of Kapton. A self passivating, self healing silica layer protecting underlying Kapton upon exposure to AO may result from the nanodispersion of silicon and oxygen within the polymer matrix. Polyhedral oligomeric silsesquioxane (POSS) is composed of an inorganic cage structure with a 2:3 Si:O ratio surrounded by tailorable organic groups and is a possible delivery system for nanodispersed silica. A POSS dianiline was copolymerized with pyromellitic dianhydride and 4,4'-oxydianiline resulting in POSS Kapton Polyimide. The glass transition temperature (T_g) of 5 to 25 weight % POSS Polyimide was determined to be slightly lower, 5 - 10 %, than that of unmodified polyimides (414 °C). Furthermore the room temperature modulus of polyimide is unaffected by POSS, and the modulus at temperatures greater than the T_g of the polyimide is doubled by the incorporation of 20 wt % POSS. To simulate LEO conditions, POSS PI films underwent exposure to a hyperthermal O-atom beam. Surface analysis of exposed and unexposed films conducted with X-ray photoelectron spectroscopy, atomic force microscopy, and surface profilometry support the formation of a SiO₂ self healing passivation layer upon AO exposure. This is exemplified by erosion rates of 10 and 20 weight % POSS PI samples which were 3.7 and 0.98 percent, respectively, of the erosion rate for Kapton H at a fluence of 8.5 x 10²⁰ O atoms cm⁻². This data corresponds to an erosion yield for 10 wt % POSS PI of 4.8 % of Kapton H. In a separate exposure, at a fluence of 7.33 x 10²⁰ O atoms cm⁻², 25 wt % POSS Polyimide showed the erosion yield of about 1.1 % of that of Kapton H. Also, recently at a lower fluence of 2.03 x 10²⁰ O atoms cm⁻², in going from 20 to 25 wt % POSS PI the erosion was decreased by a factor of 2 with an erosion yield too minor to be measured for 25 wt % POSS PI.

15. SUBJECT TERMS

16. SECURITY CLASSIFICATION OF:

a. REPORT unclassified	b. ABSTRACT unclassified	c. THIS PAGE unclassified
----------------------------------	------------------------------------	-------------------------------------

17. LIMITATION OF ABSTRACT

18. NUMBER OF PAGES

19a. NAME OF RESPONSIBLE PERSON

12

properties, UV stability and IR transparency. It is also used in conjunction with Teflon FEP in multilayer insulation blankets for thermal control insulation because of its superior optical properties, including low solar absorptance. In these multilayer insulation blankets aluminium (or gold) is typically applied to Kapton due to its low emissivity.

Over the last twenty years, it has been well established through space-based experiments and ground simulations that polymeric materials and films undergo severe degradation as a result of the aggressive environment encountered in low Earth orbits (LEO).[1-6] In this high vacuum environment, materials are subjected to the full spectrum of solar radiation and must endure constant thermal cycling from -50°C to 150°C and bombardment by low and high-energy charged particles as well as high incident fluxes of AO.[7] These harsh conditions, combined with the need for lighter weight and lower cost man-made orbiting bodies, necessitate the design of space-survivable materials.

Hybrid inorganic/organic polymers have the potential to meet the requirements of space-survivable materials by bridging the gap between ceramics and plastics by incorporating the components of silica into polymer matrices at the nanolevel. This concept of space survivability entails the erosion of organic materials by the energy provided by AO attack, the addition of AO to POSS moieties, and the subsequent formation of a silica passivation layer. Due to the naondispersion of Si and O within the polymer matrix, both a self passivating and self healing properties are expected of POSS Polyimides.

This paper presents a characterization study of POSS-containing polyimides including surface characterization before and after exposure to AO and dynamic thermal mechanical testing of unexposed polyimide films. The changes in the surface topography due to AO exposure were measured using atomic force microscopy, and the exposed surfaces were characterized using X-ray photoelectron spectroscopy. In addition, the atomic oxygen erosion rates were calculated using stylus surface profilometry.

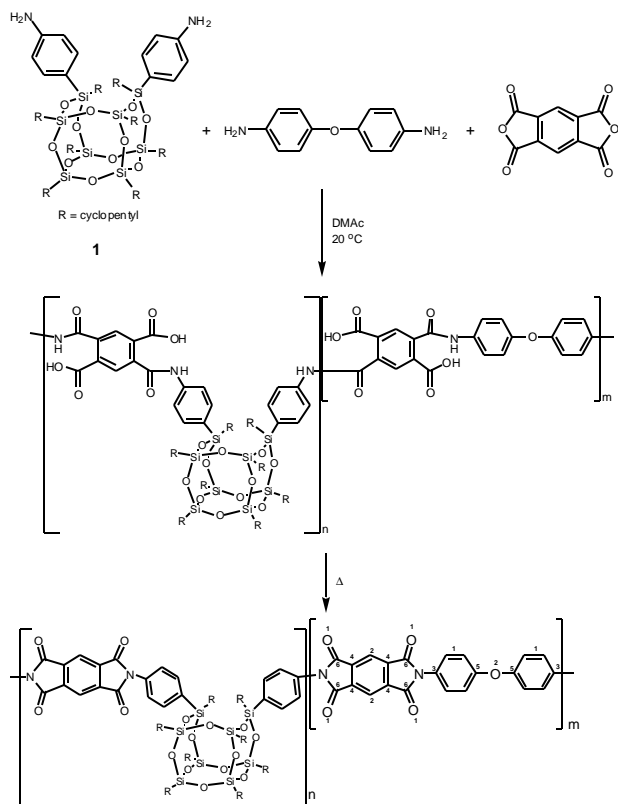
EXPERIMENTAL

Synthesis of POSS Polyimide Copolymers

Polyimides with the same chemical formula as Kapton were synthesized by using condensation polymerization of 4,4'-oxydianiline (ODA) and pyromellitic dianhydride (PMDA) in an N,N'-dimethylacetamide (DMAc) solvent[8]. A POSS framework (Figure 1) with two aniline pendant groups was synthesized using a procedure described by Prof. Frank Feher in 2003 [9]. Using this monomer, POSS-polyimide random copolymers were synthesized as shown in Figure 1 with POSS loadings corresponding to 0, 5, 10, 20, and 25 wt%.

AO Exposure of POSS Polyimides

Polyimide sample exposures were performed with a pulsed beam, operating at a repetition rate of 2 Hz and containing hyperthermal atoms that were generated with the use of a laser-detonation source [10-13]. The hyperthermal beam contains neutral atomic and molecular oxygen, with an ionic component of 0.01%. The mole fraction of atomic oxygen in the beam was approximately 70%. Prior to exposure, samples were covered with a stainless steel mesh disk in order to mask areas and achieve etched and unetched portions. Each beam pulse contained an average $1.7 \pm 0.1 \times 10^{15}$ O atoms, with a mean translational energy of 4.9-5.0 eV.



1. Synthesis of POSS-Polyimides

Surface Characterization of POSS Polyimides

All samples were handled in ambient air after exposure prior to etch depth, surface topography, and surface chemistry measurements. [14] The average of 30 step height of the etched and unetched portions was determined by surface profilometry. These measurements were obtained with the use of a Dektak³ (Veeco Metrology Group, Santa Barbara, CA) surface profilometer. Scan lengths ranged from two to four microns, and scan speeds were slow to medium. The etched-mesh screens used to cover the samples had a wire thickness of 100 μm , with approximately square open areas that were 500 μm wide. Average step heights for the masked samples were obtained from 30 different step height measurements on each sample

Atomic force microscopy was performed using a MultiMode Nanoscope III (Digital Instruments, Santa Barbara, CA) in TappingModeTM with silicon tips with a resonant frequency of approximately 300 kHz and a scanning rate in the range of 0.5 to 1 Hz.

XPS spectra were obtained with the use of non-monochromatized Mg K α radiation (1253.6 eV) and a hemispherical CLAM 2 (VG Microtech) analyzer. Sample charging shifted the XPS lines to higher binding energies by 0.5 to 3 eV. In the present study, this shift was corrected by assuming that the binding energy of the lowest C(1s) component is 285.0 eV for the unexposed polyimide (0

wt% POSS) sample. (Note that the binding energy scale was calibrated with the use of an Ag($3d_{5/2}$) line at 368.25 eV as a reference.)

Thermal and Mechanical Properties of POSS-Polyimides.

The cast films were cut into 3 x 20 mm rectangular samples for dynamic mechanical thermal analysis utilizing a DMTA V from TA Instruments. All polyimide samples were analyzed using a 5°C/min temperature ramp from room temperature to 500°C and a tensile geometry. Stress/strain tests were performed on all samples to identify the largest force in which the material exhibited an elastic deformation, thus limiting the pretension force used to test the samples. Strain sweeps were performed to ensure that the testing strain was within the linear viscoelastic region.

RESULTS AND DISCUSSION

Profilometry and Atomic Oxygen Etching Experiments

Samples of POSS-Polyimide (POSS R group is cyclopentyl) films underwent a series of AO etching experiments where they were exposed to a hyperthermal O-atom beam produced by a 7 Joule per pulse CO₂ laser source. This AO source has been well characterized and described previously [15]. The resultant beam consists predominantly of fast neutrals, with a very small ionic fraction ($<10^4$). Average kinetic energies of the fast species in the beam can range from 2 to 15 eV. A protective screen was placed in-between the sample and beam path in order to selectively erode only certain portions of the samples. The difference in etch depth between the eroded and protected part of the samples was then measured using stylus surface profilometry. By measuring the difference in height between the etched and unetched portions of the polymer sample, it is possible to calculate an AO reaction efficiency (R_e) or erosion rate for the material for a given flux. [1]

Profilometry measurements for the Kapton H standard and a 10 wt% POSS-Kapton polyimide sample were taken after a total fluence of 8.47×10^{20} atoms/cm². (1×10^{20} O Atoms/cm² is roughly equivalent to a spacecraft operating at 500 – 600 km orbit during nominal solar activity conditions for periods of at least one year. [16]) This fluence is based on the etch depth of the Kapton H reference sample (25.4 microns, 1 mil) which has an accepted erosion yield, R_e , of 3.00×10^{-24} cm³/atom. [11]. Under the same conditions, the 10 wt% POSS-Kapton polyimide etched on average only 2.2 microns (0.086 mil) corresponding to a R_e of 2.56×10^{-25} cm³/atom. It is interesting to note that this full order of magnitude improvement in atomic oxygen reaction efficiency is brought about by addition of only 10 wt % (approximately 2 mole %) POSS copolymerized in the polymer matrix. . For an assumed random polymerization this is about 1 POSS monomer per 50 monomers or 25 repeat units.

In other work a commercially available Kapton H standard, 0, 10, and 20 wt % POSS Polyimides were exposed to a smaller AO fluence of 2.62×10^{20} atoms/cm². Profilometry measurements of these samples reveal a full order magnitude improvement in the atomic oxygen reaction efficiency obtained from addition of 10 wt% POSS, while addition of 20 wt% POSS improved the reaction efficiency by 22.5 times. [17,18]

The superior performance of polyimides containing POSS is further highlighted by atomic force microscopy images before and after exposure to AO. AFM images of 0, 10, and 20 wt% POSS polyimide films that were exposed to various numbers of hyperthermal O-atom beam pulses are shown in Figure 2. These images reveal that the root mean square surface roughness increases dramatically from 2.48 nm to 126 nm for the Kapton control sample after AO exposure from 0 to 4.1×10^{20} O atoms. In contrast, the surface roughness of polyimides with POSS only increases from 2.47

DISTRIBUTION A. Approved for public release; distribution unlimited.

to 78.9 nm and from 2.86 to 39.1 nm for the 10 wt% and 20 wt% POSS, respectively. The AO reaction efficiency, $3.00 \times 10^{-24} \text{ cm}^3/\text{atom}$, of the Kapton H standard may be used to calculate the Kapton equivalent fluence and erosion yields of each exposure. For each exposure in Figure 2, the step heights (or etch depths) of POSS polyimide film are plotted as a function of the step height of the Kapton H film in Figure 3 (top) The derivative plot in Figure 3 (bottom) gives the rate of change of the step height of POSS polyimide films as a function of exposure. The derivative functions indicated that the 10 and 20 wt% POSS polyimide films reached erosion rates of 3.7 and 0.98%, respectively, of the erosion rate for Kapton H after 395,000 beam pulses ($8.47 \times 10^{20} \text{ atoms cm}^{-2}$). These results support the formation of a passivating and self-healing silica layer that is formed as a result of the nanodispersed POSS moieties reacting with AO.

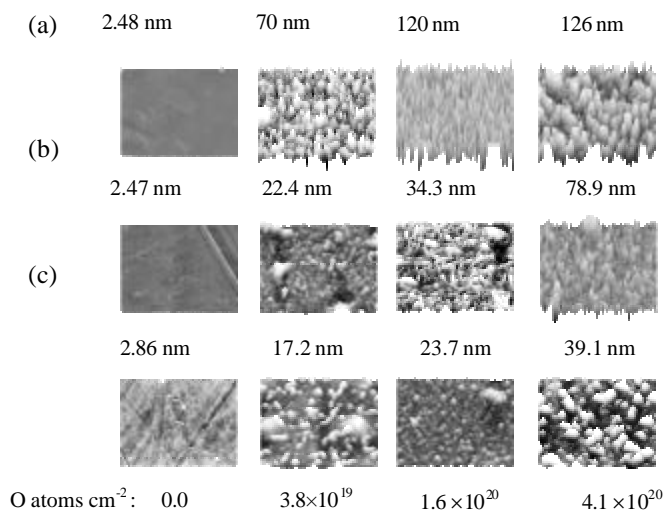


Figure 2. Atomic Force Microscopy images of POSS Polyimides with increasing atomic oxygen flux. (a) 0 wt %, (b) 10 wt % and (c) 20 wt % POSS Polyimide surfaces after exposure to atomic oxygen fluences of 0.0, 3.8×10^{19} , 1.6×10^{20} , and $4.1 \times 10^{20} \text{ O atoms cm}^{-2}$. The z scales for all images are the same, with a full scale of 500 nm. Root mean square roughness values are shown above each corresponding image.

XPS Analysis after Exposure to an Atomic Oxygen Source

X-ray Photoelectron Spectroscopy (XPS) probes the top 10 nm of the film surface. The surface layer of 10 and 20 wt% POSS-Polyimide film has been characterized using XPS before and after incremental exposures to the hyperthermal O-atom source.[19] Details of this study were described by Minton et al. [14] XPS survey spectra of C(1s) and Si(2p) peaks were obtained from 0, 10, and 20 wt% POSS-polyimide surface before and after AO exposures, and the Si(2p) spectra are shown in Figure 4. Following exposure of 20wt% POSS polyimide to 100 kpulses of the O-atom beam, the Si(2p) peak shifted from a binding energy of 102.3 eV corresponding to the silsesquioxane (Si_2O_3) to 104 eV approximately corresponding to the formation of SiO_2 .

XPS survey spectra of C(1s) and Si(2p) peaks were obtained from 0, 10, and 20 wt% POSS-polyimide surface before and after AO exposures, and the Si(2p) spectra are shown in Figure 4. Following exposure of 20wt% POSS polyimide to 100 kpulses of the O-atom beam, the Si(2p) peak

shifted from a binding energy of 102.3 eV corresponding to the silsesquioxane (Si_2O_3) to 104 eV approximately corresponding to the formation of SiO_2 . Table 1 shows a summary of XPS data for 0, 10, and 20 wt% POSS polyimide films. For 0% POSS polyimide, the oxygen concentration approximately doubled, with a greater increase in the POSS Polyimides. More importantly, in the POSS polyimides the silicon concentration reached values of 25 % and at the highest AO fluence the Si:O ratio was approximately 1:2 supporting the formation of a silica layer. [14] These surface changes are presumably responsible for the reduced erosion rates and improved AO reaction efficiencies.

Recently, the exposure of 25 wt % POSS Polyimide to 2.03×10^{20} O atoms cm^{-2} showed continued resistance to erosion with increased POSS content. Due to the very low erosion combined with sample roughness, the step height of erosion of 25 % POSS Polyimide was not measurable, but is less than the minimum measurable step height $0.15 \mu\text{m}$. The estimated erosion ratio of POSS Polyimide to 0 % POSS Polyimide for 20 wt % POSS Polyimide at 2.03×10^{20} O atoms is 0.046, and that for 25 wt % POSS is < 0.025 , showing the erosion decreased by approximately a factor of 2 with increased POSS content. A separate exposure of 25 wt % POSS Polyimide at a fluence of 7.33×10^{20} O atoms cm^{-2} , 25 wt % POSS Polyimide showed the erosion yield of about 1.1 % of that of Kapton H.

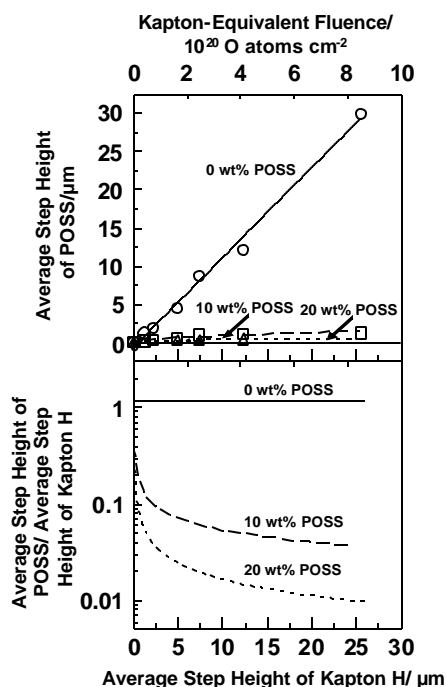


Figure 3. (top) Etch depth measurements for 0, 10, and 20 wt% POSS polyimide as a function of O-atom fluence, represented by etch depth of the Kapton H witness samples and (bottom) etch rates of POSS samples (derivatives of curves, top figure).

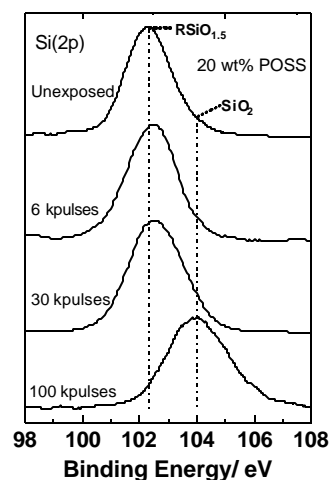


Figure 4. High resolution XPS spectra of Si(2p) line for 20 wt% POSS polyimide. 6, 30, and 100 kpulses correspond to Kapton-equivalent O-atom fluence of $\sim 1 \times 10^{19}$, 3.8×10^{19} , and 1.6×10^{20} O atoms cm^{-2} , respectively.

Table 1. Surface atomic concentrations (in percent) determined from XPS survey scans.

Sample	Exposure (beam pulses)	Kapton-equivalent atomic oxygen fluence (10^{20} O atoms cm^{-2})	C	O	Si	N
0 wt% POSS polyimide	0	0	72	19.5	1	7
	6	~ 0.1	69	20	2	9
	100	1.63	69	24	1	6
	250	4.10	55	36	0	9
10 wt% POSS polyimide	0	0	77	16	2	5
	6	~ 0.1	73	18.5	5	3.5
	100	1.63	48	30	19	3
	250	4.10	20	56	23.5	0.5
20 wt% POSS polyimide	0	0	70	20	6	4
	6	~ 0.1	66	24	7	3
	100	1.63	20	54	25	0
	250	4.10	12	60	26	1

Molecular Dynamics Modelling of POSS Polyimides

Molecular dynamics simulations may give insight to the effect of atomic oxygen on POSS polyimides. Towards this end molecular dynamics simulations of 5 eV O atom collisions with a POSS cage ($\text{Si}_8\text{O}_{12}\text{H}_8$), and with a POSS coated alkane thiol self-assembled monolayer (SAM) on a gold surface have been performed. The force field for these calculations was determined by a semi-empirical electronic structure method known as MSINDO (modified symmetrically orthogonalized intermediate neglect of differential overlap method). This is an approach which Troya and Schatz had calibrated previously [20] for O atom reactions with hydrocarbon surfaces, and in general it provides accuracy approaching density functional theory at a tiny fraction of the cost.

In studies of the reaction of O with the POSS cage, we found three reaction pathways: hydrogen abstraction to give OH plus a radical cage species (a relatively minor channel), O addition with H elimination to give H plus an oxygenated cage, and O addition with cage opening. The results of O atom collisions from 103 trajectories are given in Table 2. These results show that H elimination and cage opening (by O atom addition to the Si-O bond followed by O-O scission) are the predominant reactions with the POSS molecule. Similar mechanisms were found to apply to the studies of the POSS coated SAM. These results indicate 5 eVO atoms easily disrupt and oxidize the POSS cage. Successive reactions with O atoms, which we have not so far studied, would presumably further oxidize the POSS, ultimately to give silica.

Table 2. Molecular dynamics calculations of O(3P) collisions (5 eV) with POSS ($\text{Si}_8\text{O}_{12}\text{H}_8$) cages.

Number of trajectories	103
Impact parameter	7 a.u.*
Inelastic	63
H abstraction	3
H elimination	22
Cage opening	15

*(~Half diagonal of the Si_4 faces + 3 a.u.)

The erosion of polyimide by O atom involves the breakage and formation of various chemical bonds such as C-C, C-N, C-H, C-O and O-H bonds. Analytical force fields for O + polyimide are not available; therefore, we used direct dynamics classical trajectory method to simulate the reaction dynamics. In the direct dynamics method the classical trajectory is integrated with the forces on each atom obtained directly from quantum mechanical electronic structure calculations (MSINDO semi-empirical calculations in this case). Past studies have suggested that focus should be on the electronic ground state potential energy surface as this makes a dominant contribution to reactivity. A simplified polyimide monomer (Figure 5) structure as a model was used for the primary reaction zone and the direct dynamics calculation was carried out with this model.

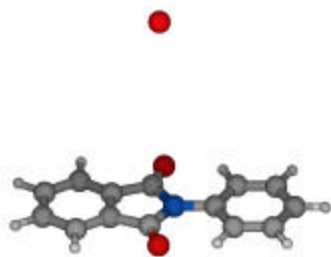


Figure 5. QM model of the primary reaction zone. Red spheres are O atoms. Gray spheres are for Carbon atoms. Blue sphere is N atom and white spheres are Hydrogen atoms.

A thousand trajectories for 5 eV O atoms colliding with the polyimide monomer in its ground state with zero point vibrational energy have been generated. Unphysical flow of the zero point energy among different vibrational modes may cause artificial dynamics behavior especially for systems with large numbers of degrees of freedom. However, this simulation, is focused on the

reactions that occur with the polyimide monomer on a very short time scale (much shorter than 1 ps), so the zero point energy flow does not influence the dynamics significantly.

The calculations found that the polyimide is very reactive (with over 67% of collisions leading to reaction). The classical trajectory simulations revealed a large number of reaction pathways but O addition reaction is found to be the dominant process. The reaction pathways have been grouped into four types: (I) Complex formation in which O is added to the monomer without breaking C-C, C-N and C-H bonds (within 1 ps); (II) O addition associated with ring-opening (C-C and C-N bond cleavage); (III) H elimination; (IV) OH abstraction. All these reactive channels are found to be exothermic (thermodynamically allowed). The branching ratios are 1: 17: 3: 3 for reaction types I-IV, respectively. Other reaction types were also observed, however they are negligible compared to the above four types of reactions.

Dynamic Mechanical Thermal Analysis (DMTA) of POSS Polyimides

The DMTA results for Kapton Polyimide show the peak of the $\tan \delta$ curve, which represents the glass transition temperature, T_g , of the polymer, at 414° C. The peak of the A series of copolymers were formulated with the oxygen in ODA replaced with cyclopentyl polyhedral oligomeric silsesquioxane forming various weight % POSS polyimides by the method described above [9]. These copolymers exhibit unique thermomechanical behavior at and above the glass transition temperature of the polymers. The $\tan \delta$ curves for all the materials mentioned above are shown in Figure 6 (bottom). One will notice in this figure a decrease in the glass transition temperature with the substitution of the POSS monomers for the ODA. This is due to ineffective packing of the polymer chains due to the incorporation of the bulky POSS molecules in the polymer backbone. One will also notice a substantial decrease in the intensity and an increase in the breadth of the loss tangent peak for the samples fabricated with 20 and 25 wt% of the ODA being replaced by the POSS monomer. The intensity of the $\tan \delta$ at T_g is a measure of the energy-damping characteristic of a material, and the breadth of the $\tan \delta$ peak indicates the cooperative nature of the relaxation process of the polymer chains. The idea of cooperativity is related to the ease at which polymer chains move at T_g . If the polymer chains in a material resist movement at T_g , then the $\tan \delta$ peak will be broad. [21-24] For the case of the 20 and 25% POSS polyimides, the increased breadth of the $\tan \delta$ peak may be a consequence of the additional volume occupied by the POSS molecules which leads to an increased steric barrier for the cooperative chain movements at T_g . The decrease in the intensity of the $\tan \delta$ peak indicates that the material is not effective in dissipating energy and thus would be a poor impact-resistant material.

Figure 6 (top) illustrates the elastic modulus of the materials in the rubbery plateau region, temperatures above the T_g of the material. One will first notice the incorporation of the POSS monomer in the polyimide increases the modulus in this temperature regime. The magnitude of the modulus in this region is inversely proportional to the molecular weight between entanglements or the number of cross-links [25]. If one sees a large increase in the modulus in this region, as is seen in the data for 20 wt% POSS polyimide in Figure 6 (top), it is indicative of the presence of a cross-linking reaction during the testing. Such a reaction is known to occur at high temperatures for polyimides formed with PMDA and ODA monomers. The mechanism of the reaction is believed to be a cleavage of the imide ring and the recombination with another polyimide chain, thus creating a cross-linked network [26]. One will notice that the substitution of the POSS monomer retards this reaction, as is evident in the smaller magnitude increase in the elastic modulus; but the POSS provides a reinforcing mechanism which ultimately results in an increased modulus in the rubbery regime. It is also significant to note that the addition of 25 wt% shows a lower modulus, indicating that there is an optimal amount of POSS required to maximize this reinforcement .. The hindrance of

the reaction may be due to a steric effect caused by the size of the POSS molecule, 1.5 nm, as opposed to an oxygen atom, 73 pm. The larger molecule in the polymer backbone will create a barrier, in which a second polyimide chain may not be able to properly conform in order to complete the cross-linking reaction. The optimum may be a result of POSS agglomerates reaching a critical size and aiding in the interactions between polymer chains. This hypothesis is presently under investigation. The complete imidization of these materials is currently under investigation.

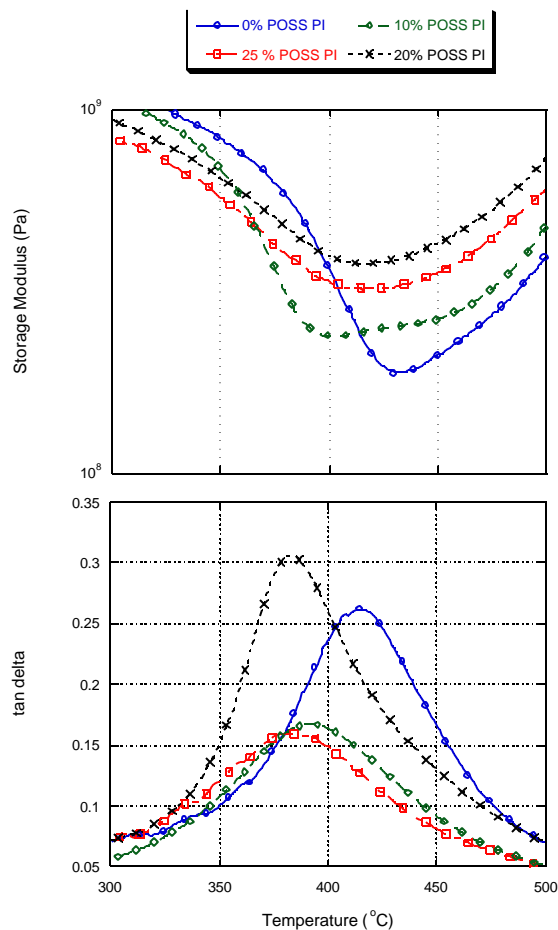


Figure 6. (top) Storage modulus for POSS polyimides in the rubbery plateau region and (bottom) tangent delta curves for 0, 10, 20 and 25 wt% POSS polyimides.

CONCLUDING REMARKS

The incorporation of POSS nanostructures into polyimides should significantly extend the usable lifetime of these materials in LEO applications. Comparative erosion yields following exposure to an

atomic oxygen source show that POSS polyimides exhibit a significantly improved oxidation resistance. XPS data and molecular dynamics simulations support that this is due to a rapidly formed self-passivating and self-healing silica layer upon exposure of POSS Polymers to high incident fluxes of atomic oxygen. The incorporation of the POSS does slightly reduce the glass transition temperature, but the modulus in the rubbery plateau region is greatly enhanced. The physical characteristics will be revisited after thermal cycling in the future. This technology could be easily adapted to other polymeric systems, such as structural polymers like polyethylene and polypropylene, revolutionizing the field of space-survivable materials.

ACKNOWLEDGEMENTS

The authors would like to thank Mr. Scott Barker for performing the dynamic mechanical thermal testing. This work was financially supported by the Air Force Office of Scientific Research (Grant No. F49620-01-1-0276) and from the Air Force Office of Scientific Research through a Multiple University Research Initiative (Grant No. F49620-01-100335).

REFERENCES

1. de Groh, K. K., Banks, B. A., "Techniques for Measuring Low Earth Orbital Atomic Oxygen Erosion of Polymers," 2002 Symposium and Exhibition sponsored by the Society for the Advancement of Materials and Process Engineering, Long Beach, CA, May 12-16, 2002.
2. Koontz, S. L., Leger, L. J., Visentine, J. T., Hunton, D. E., Cross, J. B., and Hakes, C. L., "EOIM-III Mass Spectroscopy and Polymer Chemistry: STS 46, July – August 1992," *Journal of Spacecraft and Rockets*, Vol. 32, No. 3, 1995, pp. 483 – 495.
3. de Groh, K. K., and Banks, B. A., "Atomic-Oxygen Undercutting of Long Duration Exposure Facility Aluminized-Kapton Multilayer Insulation," *Journal of Spacecraft and Rockets*, Vol. 31, No., 4, 1994, pp. 656 – 664.
4. Banks, B. A., Rutledge, S. K., de Groh, K. K., Mirtich, M. J., Gebauer, L., Olle, R., and Hill, C. M., "The Implication of the LDEF Results on Space Freedom Power System Materials," *Proceedings of the 5th International Symposium on Material in a Space Environment*, Cannes-Mandelieu, France, 1991, p. 137
5. Tennyson, R. C., "Protective Coatings for Spacecraft Materials," *Surface and Coatings Technology*, 68/69 (1994) 519 – 527. p.45.
6. Gilman, J.W., Schlitzer, D. S., Lichtenhan, J. D., "Low Earth Orbit Resistant Siloxane Copolymers," *Journal of Applied Polymer Science*, Vol. 60, p. 591 – 596. (1996)
7. Grobner, J. and Kerr, J. B., "Ground-Based Determination of the Spectral Ultraviolet Extraterrestrial Soalar Irradiance: Providing a Link Between Space-Based and Ground-Based Solar UV Measurements," *Journal of Grophysical Research-Atmospheres*, 2001. 106(D7): p. 7211 - 7217.
8. Mather, P.T., Jeon, H.G., Romo-Urbe, A., Haddad, T.S., and Lichtenhan, J.D., "Mechanical Relaxation and Microstructure of Poly(Norbornyl- POSS) Copolymers," *Macromolecules*, 1999. 32(4): p. 1194-1203.
9. Wright, M. E., Schorzman, D. A., Feher, F.J., and Jin, R. Z., "Synthesis and Thermal Curing of Aryl-Ethynyl-Terminated coPOSS Imide Oligomers: NewInorganic/Organic Hybrid Resins," *Chemistry of Materials*. 2003, 15, 264-268
10. Feher, F.J., Nguyen, F., Soulivong, D., and Ziller, J.W., "A New Route to Incompletely Condensed Silsesquioxanes: Acid-Mediated Cleavage and Rearrangement of (c-C₆H₁₁)(6)Si₆O₉ to C-2-[(c-C₆H₁₁)(6)Si₆O₈X₂]," *Chemical Communications*, 1999(17): p. 1705-1706.

DISTRIBUTION A. Approved for public release; distribution unlimited.

11. Feher, F.J., Terroba, R., and Ziller, J.W., "A New Route to Incompletely-Condensed Silsesquioxanes: Base-Mediated Cleavage of Polyhedral Oligosilsesquioxanes," *Chemical Communications*, 1999(22): p. 2309-2310.
12. Feher, F.J., Soulivong, D., and Eklund, A.G., "Controlled Cleavage of $R_8Si_8O_{12}$ Frameworks: A Revolutionary New Method for Manufacturing Precursors to Hybrid Inorganic-Organic Materials," *Chemical Communications*, 1998(3): p. 399-400.
13. Blanski, R.L., Phillips, S. H., Chaffee, K., Lichtenhan, J. D., Lee, A., and Geng, H.P., "The Preparation and Properties of Organic/Inorganic Hybrid Materials by Blending POSS into Organic Polymers," *Polymer Preprints*, 2000. 41(1): p. 585.
14. Amy L. Brunsvold, Timothy K. Minton*, Irina Gouzman, Eitan Grossman, and Rene Gonzalez *The Journal of High Performance Polymers*, Special Edition, Publication, 2004, 16(2), p.303-318.
15. Gonzalez, R. I., "Synthesis and In-Situ Atomic Oxygen Erosion Studies of Space-Survivable Hybrid Organic/Inorganic POSS Polymers," Ph.D. Dissertation, Chem Eng Department, University of Florida, 2002. <http://purl.fcla.edu/fcla/etd/UFE1000127>
16. Gonzalez, R. I., Phillips, S. H., Hoflund, G. B., "In Situ Oxygen-Atom Erosion Study of polyhedral oligomeric silsesquioxane-Siloxane Copolymer," *Journal of Spacecraft and Rockets*, 2000, 37(4), p.463 -467.
17. Minton, T. K., and Garton, D. J., "Dynamics of Atomic-Oxygen-Induced Polymer Degradation in Low-Earth Orbit," in *Advanced Series in Physical Chemistry: Chemical Dynamics in Extreme Environments*, edited by R. A. Dressler (World Scientific, Singapore, 2001), pp. 420-489.
18. Dooling, D. and Finckenor, M. M., "Material Selection Guidelines to Limit Atomic Oxygen Effects on Spacecraft Surfaces, NASA/TP – 1999 -209260, p.
19. Garton D J, Minton T K, Maiti B, Troya D, and Schatz G C 2003 *Journal of Chemical Physics* 118 1585-8
20. Diego Troya and George C. Schatz, *J. Chem. Phys.*, 120, 7696-7707 (2004).
21. Cornelius, C.J. and E. Marand, *Polymer* 2002; 43: 2385.
22. Mauritz, K.A. and M. Warren, *Macromolecules* 1989; 22: 1730.
23. Matos, M.C., L.M. Ilharco and R.M. Almeida *J Non-Cryst Solids* 1992; 147,148: 232-7.
24. Cowie J.M.G. *Polymers: chemistry and physics of modern materials. 2nd Ed.* New York: Blackie/Chapman & Hall, 1994.
25. Menard, K.P. *Dynamic Mechanical Analysis: A Practical Introduction* New York: CRC Press, 1999.
26. Adrova, N.A., M.I. Bessonov, L.A. Laius and A.P. Rudakov *Polyimides: A New Class of Heat-resistant Polymers* Jerusalem: IPST Press, 1969